THE DYNAMIC RESPONSE OF A CHILD'S THORAX TO BLUNT TRAUMA.

Introduction

The effects of blunt trauma to the chest of a child can be scientifically studied experimentally using volunteers, cadavers or anthropometric dummies or by mathematical simulation. All have conceptual and practical limitations. Mathematical modeling is the most versatile since it enables one to conduct parametric studies to determine the relative effects of a variety of factors. It does, however, require considerable quantitative data for its construction. The geometry of the bony thorax, the mass distribution of the skeleton and viscera, the nature of the constraints provided by the variety of joints, the constitutive properties of the materials are some of the categories of required information. To date, much of this is unavailable in the literature and as a consequence the majority of modeling efforts have been limited to lumped parameter descriptions (e.g. 1)*.

Recent studies (2,3,4) have shown how some of the fundamental geometric information can be obtained and that finite element modeling of the thorax is a promising tool in the study of blunt chest trauma.

In this brief paper we will present some recent results obtained from our three-dimensional dynamic finite element model of a child which we have designated THORAX III-C.

The THORAX III-C Model

The THORAX III-C model is a midsagittally symmetric finite element representation of the thoracic skeleton of a "child." The anthropometric characteristics were obtained in part by direct measurements from a commercially available articulated child's skeleton estimated to be 7 to 8 years of age. Certain of the global geometric measurements (e.g., orientation of the ribs) were subsequently modified to correct for obvious discrepancies incurred during assembly of the skeleton. The corrections were accomplished through the use of anatomical descriptions available in the literature (e.g., 5) and by observations and measurements made during a disection of a 9 year old male cadaver.**

THORAX III-C consists of a collection of 157 discrete, three dimensional, elastic, beam elements representing the ribs, vertebrae, intervertebral discs, costal cartilage and sternum (Fig. 1). Each is capable of transmitting 6 components of force and moment. The assemblage of these elements forms a model of the thoracic skeletal system having a total of 149 nodal points, 759 degrees of freedom and the following approximate anthropometric characteristics.

---

*Numbers in parentheses refer to references listed at end of paper.

**Through the generosity and cooperation of Drs. E. Eldred and B. Towers, UCLA School of Medicine.

Sternum length									3 in.*	
Costae	1	2	3	4	5	6	7	8	9	10
Length (in.) (Head to SCJ)	2	4.5	5.5	6.8	7.0	7.0	6.5	6.0	5.5	4.5
Vertebral Column (C-1 to L-5)									12 in.	
Max. Lateral Dimension (at Midaxilla)									5 in.	
Max. A-P Dimension (Stern. to V.C.)									3 in.	
Weight of THORAX									26 lbs.	

The Elements

The dimensions of the major and minor cross-sectional principal axes of inertia of the individual ribs were measured from the skeleton at numerous points along each rib. The cross-sectional properties were calculated (Table 1) using the procedure developed in (2) and the assumed compact bone to total cross-sectional area ratios (A_c/A_T) shown in column 2. The cross-sectional dimensions of the costal cartilages were assumed constant for each costa and taken as those of the ribs at their costochondral junctions (CCJ).

TABLE 1

Selected Rib Cross-Sectional Properties (at Midaxilla)

		Measured Dimensions		Calculated Quantities**			
Rib No.	$\frac{A_c}{A_T}$	Maj. Axis (in.)	Minor Axis (in.)	A_c (in^2)	I min $\times 10^5$ (in^4)	I max $\times 10^5$ (in^4)	J $\times 10^5$ (in^4)
1	0.6	0.34	0.07	0.013	0.61	9.4	0.20
2	0.55	0.33	0.09	0.017	1.04	10.6	0.33
3	0.45	0.31	0.14	0.026	3.10	12.6	0.88
4	0.4	0.29	0.16	0.028	3.70	10.2	0.96
5	0.4	0.18	0.16	0.027	3.66	9.6	0.94
6	0.4	0.30	0.17	0.031	4.85	12.8	1.25
7	0.4	0.33	0.14	0.029	3.42	13.7	0.98
8	0.4	0.38	0.11	0.026	1.87	15.3	0.62
9	0.4	0.40	0.60	0.023	1.24	14.2	0.42
10	0.4	0.51	0.80	0.015	0.48	4.6	0.17

The superior surface of each rib shaft was observed to be essentially planar, which coincides with previous findings (3). Consequently, the elastic axis of each rib was defined by two planar circular arcs, from the head to the angle and from the angle to the CCJ. The elastic axis was located half-way

*See last page for conversion to S-I units.
**I = moment of inertia, J = Torsion constant.

between the superior and inferior borders of each rib. The "twisting" of the minor principal axis of inertia was similar to that previously observed (3) and was similarly modeled. Ten elements were used to model each costa (Fig. 1).

The sternum varied in width from 1 in. at the manubrium to 0.53 in. at mid-height of the body. It was modeled using 13 beam elements (Fig. 2) having cross-sectional properties calculated from the gross sternum dimensions.

The dimensions of the vertebral bodies and the intervertebral discs were measured directly from the skeleton and the cross-sectional properties calculated as in (4). The relative positions of the vertebra and the consequent spinal curvatures appeared reasonable. Each vertebra and disc was modeled as a beam element.

Mass Distribution and Material Properties

The mass of the THORAX III-C model (26 lbs.) was uniformly distributed to the nodal points (Fig. 1) along the elastic axes of each of the upper 10 ribs. The rotary inertia of all elements except the head was neglected and the mass below T-10 was lumped at discrete points along the vertebral column.

Element materials were appropriately characterized as either compact bone or cartilage. Both were assumed to be Hookean (6) with E* (bone) = 1.75×10^6 psi, G (bone) = 0.73×10^6 psi, E (cart.) = 40,000 psi and G (cart.) = 18,500 psi.

Solution Method and Natural Modes

The small deformation stiffness and mass matrices were calculated for each element and compatibly assembled to form the system equations of motion using SAP IV (7). The mode shapes and frequencies were calculated by the determinant search method. The first 20 frequencies are tabulated below.

Mode No.	1	2	3	4	5	6	7	8	9	10
Frequency (Hz)	4.8	5.9	8.0	8.5	10.8	14.4	15.3	16.4	17.5	18.9
Mode No.	11	12	13	14	15	16	17	18	19	20
Frequency (Hz)	19.2	23.1	24.0	24.7	25.8	26.1	27.3	27.6	28.6	29.1

The first mode (4.8 Hz) represents whole body cantilever, A-P displacement and rotation about the fixed end of the lumbar spine (N.P. 149, Fig. 1). The second, third and fourth modes (5.9 to 8.5 Hz) produce local motion in the cartilage of the lower ribs. The intermediate modes appear to generate flexural and torsional motion of the ribs whereas the relatively stiff sternum responds in the higher modes.

An examination of the mode shpaes revealed that except for the first few lowest frequency modes the remainder are highly coupled and cannot be simply characterized. Efforts are under way to systematically sort out their dominant features to aid in further characterizing the dynamics of the human thorax.

---

*E = Modulus of Elasticity, G = Shear Modulus

Forced Response

The THORAX III-C model can be exercised by applying distributed (temporally and spatially) midsagitally symmetric forcing functions to a selected set of nodal points. The response can be calculated by modal superposition of the uncoupled system or by direct integration of the coupled equations of motion.

The particular forcing function chosen for this study was a triangular pulse in the anteroposterior (-X) direction, having a peak amplitude of 240 lbs. (to entire chest) at 20 ms, a duration of 40 ms and an input impulse of 4.8 lb.-sec. The magnitude was chosen to be approximately 20% of that observed in experiments on adult cadavers (1). Since the model is linear, the results can be proportionaly scaled to any desired amplitude. The load was distributed to nodal points 13, 24, 26, 37, 50, 63, 78 and 92 (Fig. 2) simulating application through a 3.5 in. diameter strike centered mid-sternally at R-6 (N.P. 52).

The X displacement-time response of 3 points along the midsternal line relative to the vertebral column is shown in Fig. 3. During the first 30 ms, the sternum translates essentially as a rigid body. Somewhat abruptly at 30 ms there is a change in the displacement field. The superior region of the sternum having achieved its maximum displacement begins to return to its equilibrium position whereas the inferior section continues to move in the direction of the applied load.

This is also illustrated in Fig. 4 which shows the motion of the sternum relative to the vertebral column in the midsaggital plane. The higher frequency response of the manubrium is attributed to the relatively large stiffness presented by rib 1. The lagging response of the lower end of the sternal body is a result of the very flexible restraints provided by the cartilage of ribs 7 through 10. Consequently, the maximum penetration of the sternum into the thorax will be achieved at the xiphisternal junction.

As expected, the midaxillary line displaces posteriorly and laterally in the +Y direction. The 6th, 7th and 8th ribs experience the largest lateral displacements of 0.34, 0.7 and 1.2 inches. respectively, occurring at approximately 46 ms.

A plot of the normalized applied force as a function of relative sternum X displacement is shown in Fig. 6. We observe that the maximum displacement lags behind the force and that in the upper sternum (R-1 to R-3) this produces a "hysteresis" type effect which in THORAX III-C is a result of variations in stiffness rather than by some form of energy dissipation.

To help put these results into some perspective, a curve representing the "average" adult data reported in (8) has been superimposed on the THORAX III-C curves in Fig. 6. For numerous reasons, no direct comparison will be attempted.

Conclusions

THORAX III-C is a structural dynamic simulation of a "child's" thorax. With the paucity of quantitative anthropometric information available no attempt was made to statistically represent a child's thorax. The conclusions, therefore, must be considered as indicative rather than quantitatively representative of all children.

The lowest natural mode which produces deformation of the rib cage occurs at approximately 7 Hz and represents motion of the flexible cartilage of the lower ribs. The ribs and sternum begin to respond at about 10 Hz with the sternum becoming quite active above 20 Hz. The frequencies (f) are approximately related to mode number (M) bilinearly. Up to 20 Hz, $f \simeq 2M$, whereas from 20 Hz to 30 Hz $f \simeq 0.8M$.

In response to a triangular pulse the anterior chest wall displaces posteriorly and inferiorly with the xiphisternal junction experiencing the maximum penetration into the thorax. The anterior ends of the ribs follow the sternum and the midaxillary line moves laterally.

The force-displacement characteristic of the sternum is not unlike that observed in adult cadaver tests (8), nor those obtained from impact tests on the Rhesus monkey (9, 10).

The internal forces in each element of THORAX III-C were also calculated. Maximum internal stresses and estimates of potential fracture sites can thus be determined. Discussion of this, however, will be reserved for a future communication.

Considerable additional refinements and parametric studies are clearly in order. The effects of the musculature, finite deformations, the stiffness of the viscera, improved descriptions of the major joints and refinements in geometry will improve the relationship of THORAX III-C to that of an actual child.

REFERENCES

(1) Lobdell, R. E., Kroell, C. K., Schneider, D. C., Hering, W. E. and Nahum, A. M. (1972) "Impact Response of the Human Thorax," Human Impact Response Measurement & Simulation, Edited by W. F. King and H. J. Mertz, Plenum Press, New York (1973).

(2) Roberts, S. B. and Chen, P. H., (1970) "On Some Geometric Properties of Human Ribs - I," Proceedings of the Symposium on Biodynamic Models and Their Applications, Dayton, Ohio, October 26-29, 1970.

(3) Roberts, S. B. and Chen, P. H. (1972) "Global Geometry Characteristics of Typical Human Ribs," J. of Biomechanics, 5:191-201.

(4) Roberts, S. B. and Chen, P. H. (1970) "Elastostatic Analysis of the Human Thoracic Skeleton," J. of Biomechanics, 3:327-545.

(5) Anson, B. J. (1966) Morris' Human Anatomy, 12th Edition, McGraw Hill, New York.

(6) Yamada, H. (1970) Strength of Biological Material, Williams & Wilkins, Baltimore, Md.

(7) Bathe, K. J., Wilson, E. L., and Peterson, F. E. (1973) "SAP IV - A Structural Analysis Program for Static and Dynamic Response of Linear Systems," University of California, Berkeley Report No. EERC 73-11.

(8) Stalnaker, R. L., McElhaney, J. H., Roberts, V. L. and Trollope, M. L. (1972) "Human Torso Response to Blunt Trauma," Human Impact Response Measurement & Simulation, Edited by W. F. King and H. J. Mertz, Plenum Press, New York (1973).

(9) Beckman, D. L. and Palmer, M. F. (1970) "Thoracic Force-Deflection Studies in Primates," J. of Biomechanics, Vol. 3, pp. 223-227.

(10) Beckman, D. L., Palmer, M. F., and Roberts, V. L. (1970) "Thoracic Force-Deflection Studies in Living and Embalmed Primates," J. of Biomechanics, Vol. 3, pp. 551-555.

Conversion to S-I Units

1 in. = 0.0394 mm

1 lb. = 0.225 Newtons (N)

1 psi = 0.145 kN/m^2

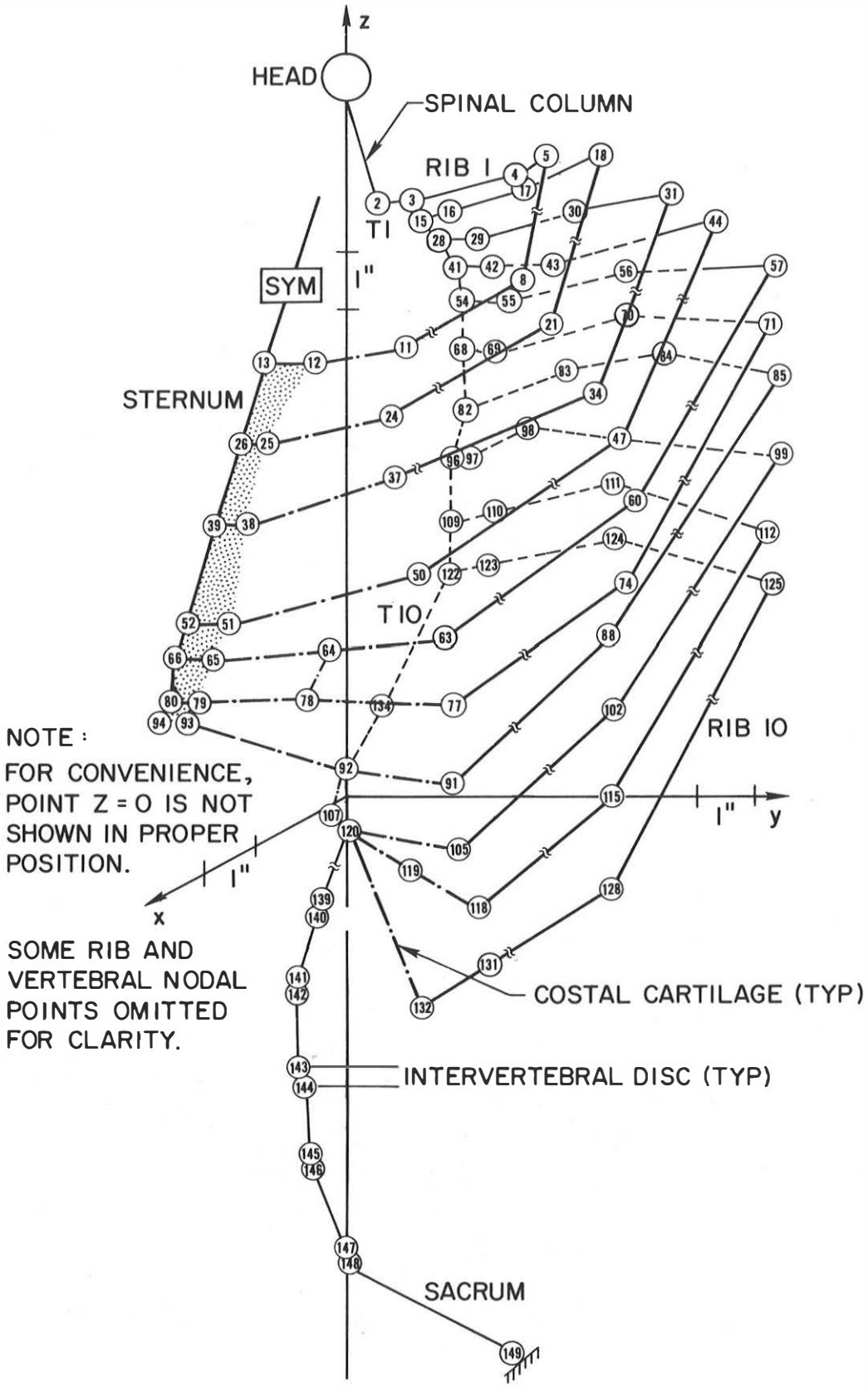

Figure 1. THORAX III-C Finite Element Model.

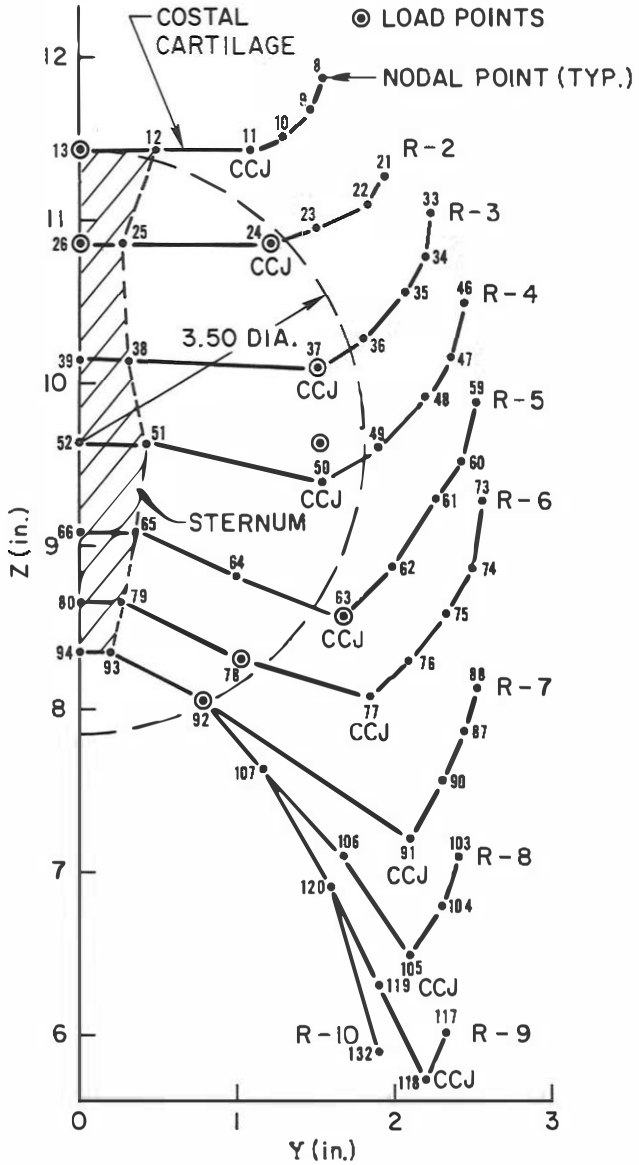

Figure 2. Local Finite Element Description of Sternum.

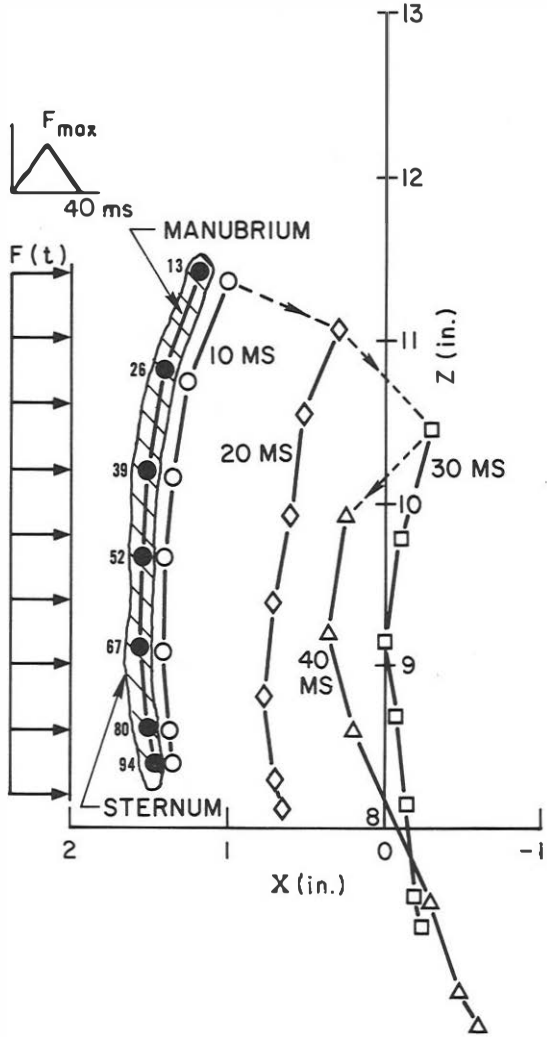

Figure 3. Midsagittal Displacements of Sternum Relative to Vertebral Column.

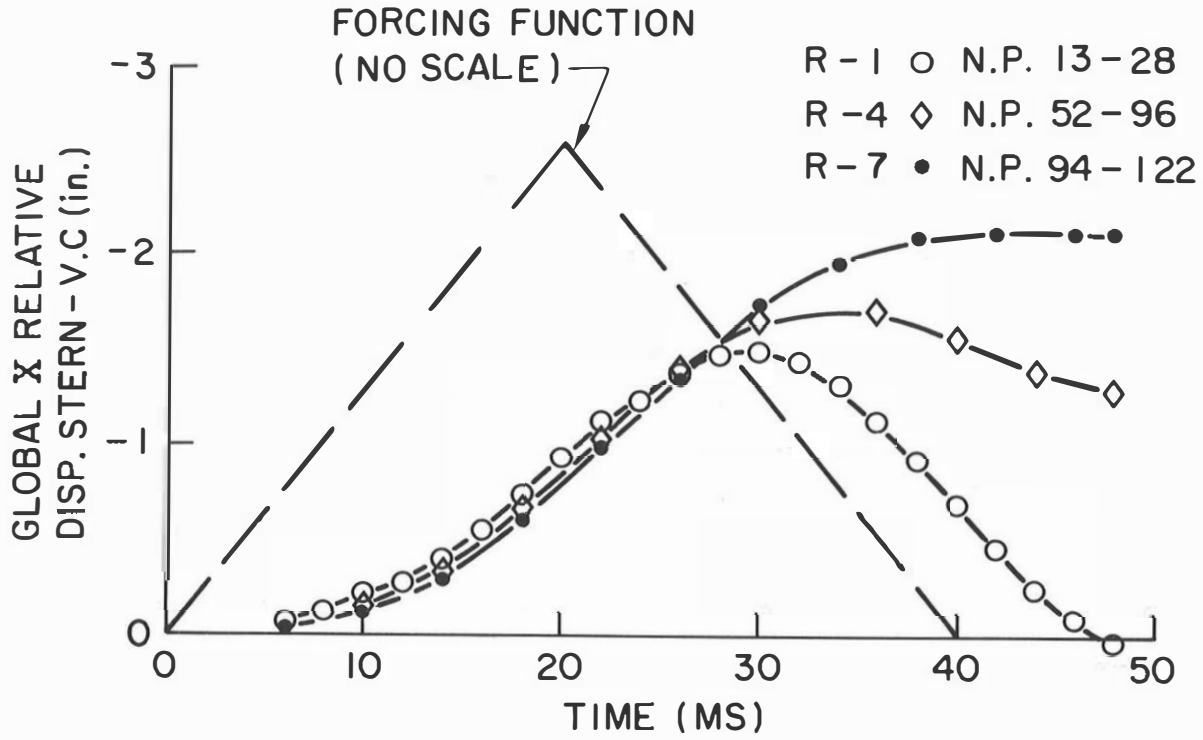

Figure 4. Relative X Displacement of Sternum vs Time.

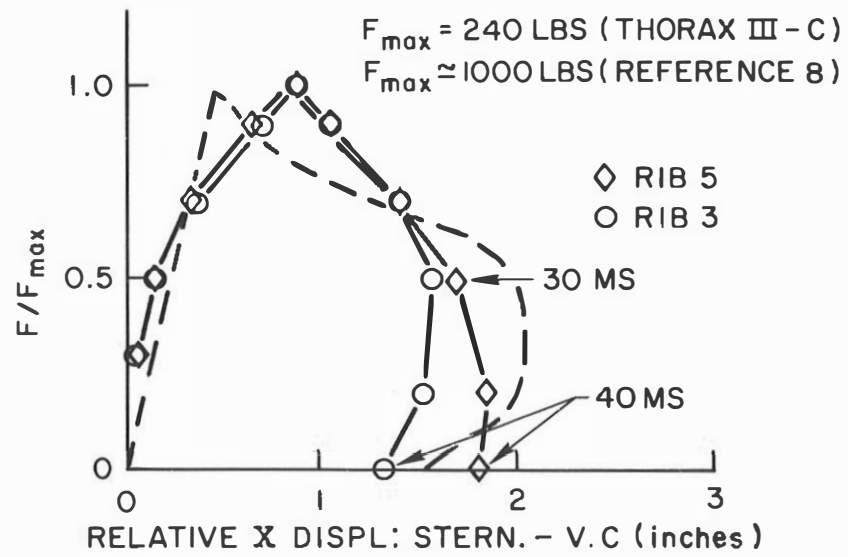

Figure 5. Normalized Force vs Relative Sternum Displacement.